ADVANCES IN ATMOSPHERIC SCIENCES, VOL. 25, NO. 3, 2008, 387–394

Prediction of the Asian-Australian Monsoon Interannual Variations with the Grid-Point Atmospheric Model of IAP LASG (GAMIL)

WU Zhiwei[1,2] (吴志伟) and LI Jianping*[1] (李建平)

[1] *State Key Laboratory of Numerical Modeling for Atmospheric Sciences and Geophysical Fluid Dynamics (LASG), Institute of Atmospheric Physics (IAP), Chinese Academy of Sciences,* 100029

[2] *Graduate University of Chinese Academy of Sciences, Beijing* 100049

(Received 3 August 2007; revised 3 December 2007)

ABSTRACT

Seasonal prediction of Asian-Australian monsoon (A-AM) precipitation is one of the most important and challenging tasks in climate prediction. In this paper, we evaluate the performance of Grid Atmospheric Model of IAP LASG (GAMIL) on retrospective prediction of the A-AM interannual variation (IAV), and determine to what extent GAMIL can capture the two major observed modes of A-AM rainfall IAV for the period 1979–2003. The first mode is associated with the turnabout of warming (cooling) in the Niño 3.4 region, whereas the second mode leads the warming/cooling by about one year, signaling precursory conditions for ENSO.

We show that the GAMIL one-month lead prediction of the seasonal precipitation anomalies is primarily able to capture major features of the two observed leading modes of the IAV, with the first mode better predicted than the second. It also depicts the relationship between the first mode and ENSO rather well. On the other hand, the GAMIL has deficiencies in capturing the relationship between the second mode and ENSO. We conclude: (1) successful reproduction of the El Niño-excited monsoon-ocean interaction and El Niño forcing may be critical for the seasonal prediction of the A-AM rainfall IAV with the GAMIL; (2) more efforts are needed to improve the simulation not only in the Niño 3.4 region but also in the joining area of Asia and the Indian-Pacific Ocean; (3) the selection of a one-tier system may improve the ultimate prediction of the A-AM rainfall IAV. These results offer some references for improvement of the GAMIL and associated seasonal prediction skill.

Key words: Asian-Australian monsoon, interannual variation, ENSO, atmospheric general circulation model, GAMIL

DOI: 10.1007/s00376-008-0387-8

1. Introduction

The dynamical model simulation and seasonal prediction of the Asian-Australian monsoon (A-AM) rainfall has been a major challenge. Many researchers investigated performances of atmospheric general circulation models (AGCMs) on various aspects of monsoons and their prediction (Sperber and Palmer, 1996; Webster et al., 1998; Wang et al., 2004a; Zhang and Li, 2007). Sperber and Palmer (1996) evaluated performances of thirty two AGCMs that participated in the Atmospheric Model Intercomparison Project (AMIP). These models show little or no predictability in the all-Indian rainfall from 1979 to 1988 except during the 1987 El Niño and the 1988 La Niña. Wang et al. (2004a) assessed performances of the ensemble simulations of A-AM anomalies in eleven AGCMs during the unprecedented El Niño period, September 1996–August 1998, and found that the summer rainfall patterns in the A-AM region (30°S–30°N, 40°–160°E) (Li and Zeng, 2003) are reproduced more poorly than its counterpart in the El Niño region. The climate variations in the tropics are determined by slow oceanic dynamical processes (Zebiak and Cane, 1987). For this reason, El Niño and the associated Southern Oscillation are perhaps the most predictable phenomenon in

*Corresponding author: LI Jianping, ljp@lasg.iap.ac.cn

the Earth climate system (Cane et al., 1986).

In spite of the above difficulties in the A-AM interannual variation (IAV) simulation and seasonal prediction, determining the predictability of A-AM IAV and identifying the sources of predictability are of central importance in seasonal prediction and forecasting the uncertainties associated with the prediction. How to determine climate predictability in a model hindcast remains elusive. We propose that the distinguished leading modes of the A-AM IAV are likely more predictable than other higher modes. These leading modes may represent the predictable part of the variability. Therefore, it is important to assess how well a climate model captures the leading modes of the A-AM IAV and to determine how the model's performances in capturing these leading modes are related to the seasonal prediction skills. This is the major purposes of the present study.

Our analysis will focus primarily on precipitation, because precipitation is the most important variable for seasonal prediction and also the most difficult variable for seasonal prediction. Examination of precipitation prediction is the most rigorous test for a climate model.

2. The model, data and methodology

The model examined here is the GAMIL which was developed in the State Key Laboratory of Numerical Modeling for Atmospheric Sciences and Geophysical Fluid Dynamics (LASG), Institute of Atmospheric Physics (IAP), Chinese Academy of Sciences (CAS). This model also participated in the "Climate Prediction and Its Application to Society" (CliPAS) project which is aimed at supporting the Asia-Pacific Economic Cooperation (APEC) Climate Center (APCC) for seasonal prediction and its application to society. The GAMIL employs a horizontal resolution of $2.8^\circ \times 2.8^\circ$ and there are 26 levels in the vertical resolution. The dynamical core is designed in LASG/IAP using the semi-implicit finite difference scheme with exact effective energy conservation, mass conservation, and terrain reduction (Wang et al., 2004b). The physical package comes mainly from the National Center for Atmospheric Research (NCAR) Community Atmosphere Model, Version 2 (CAM2), in which an improved Tiedtke convective Scheme (Tiedtke, 1989) is used to replace the original convective parameterization (Li et al., 2007).

Our analysis uses its two-tier hindcast data for the period 1979–2004 that start four times a year, targeting a 6-month prediction starting from 1 February, 1 May, 1 August, and 1 November. Note that in a two-tier approach, sea surface temperature (SST) was first predicted by using coupled models and then the atmospheric anomalies were predicted by using atmospheric models forced by the predicted SST (Bengtsson et al., 1993). The predicted SST forcing GAMIL here is taken from CliPAS project. In the present study, we will focus on evaluating the one-month lead seasonal forecast dataset. The Global Precipitation Climatology Project (GPCP) data (Adler et al., 2003) were used as a verification dataset. The observational 850 hPa wind fields are obtained from the National Centers for Environmental Prediction (NCEP)/Department of Energy (DOE) AMIP II Reanalysis (NCEP-2 henceforth) data (Kanamitsu et al., 2002) and the observational SST data are obtained from the improved Extended Reconstructed SST Version 2 (ERSST V2) data (Smith and Reynolds, 2004).

The year-to-year variation in the vast A-AM region exhibits enormous regional differences and depends strongly on season. This complexity arises from the dependence of the anomalous monsoon climate on the phases of ENSO and the phases of the annual cycle (Meehl, 1987). Based on this physical consideration, Wang and An (2005) have put forward a Season-reliant Empirical Orthogonal Function (S-EOF) analysis method to distinguish modes of variability that evolve with seasons. Their S-EOF analysis of the Indo-Pacific SST anomalies yielded two statistically significant leading modes, which are not obtainable by using conventional EOF analysis. They are the Low-Frequency (LF) and Quasi-Biennial (QB) modes which distinguish each other in their seasonal evolution, spatial structure of the fractional variance, and interdecadal variation and trend. The differences between the S-EOF and extended EOF (Weare and Nasstrom, 1982) and cyclostationary EOF (Kim, 2002) analyses were discussed in Wang and An (2005).

The purpose of the S-EOF is to depict seasonally evolving anomalies throughout a full calendar year. Here we adopt the concept of the "monsoon year" (Yasunari, 1991) from the summer, autumn and winter of year 0 [shortly JJA(0), SON(0) and DJF(0/1), respectively], to the spring of the following year (year 1), MAM (1). For this purpose, a covariance matrix is constructed using four consecutive seasonal mean anomalies for each year, i.e., treat the anomalies for JJA (0), SON(0), DJF(0/1), and MAM(1) as a "yearly block" that is labeled as year (0) in which the sequence of anomalies commences. When the EOF decomposition is done, the yearly block is then divided into four consecutive seasonal anomalies, so that one obtains a seasonally evolving pattern of the monsoon anomalies in each monsoon year for each eigenvector.

We apply the S-EOF analysis to both observed and predicted seasonal mean precipitation anomalies,

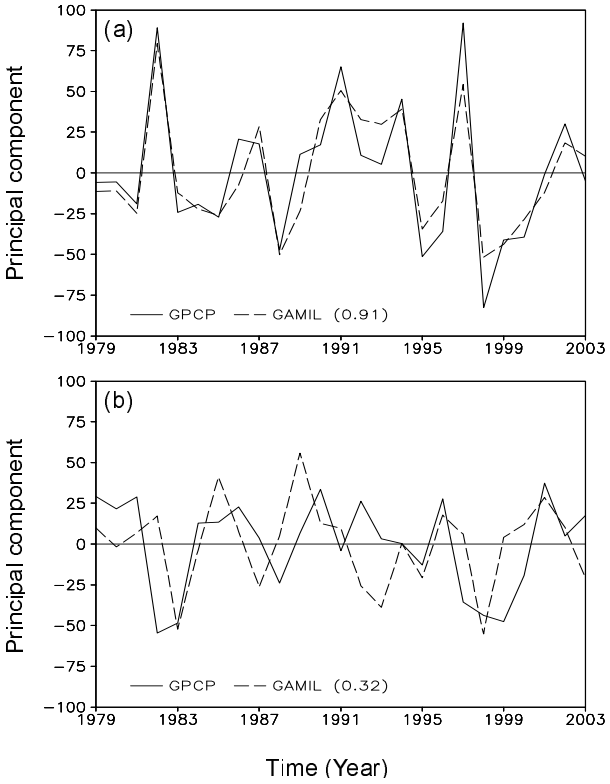

Fig. 1. Principal components of (a) the first and (b) the second S-EOF modes of seasonal precipitation anomaly obtained from GPCP observation (solid) and GAMIL prediction (dashed), respectively.

which are the departures from the mean annual cycle derived from the period 1979–2003. In the present study, we consider the A-AM region extending from 30°S to 40°N and from 40°E to 160°E, which covers South Asia and Australia as well as nearly the entire Indo-Pacific warm pool region.

Seasonal mean prediction is obtained from the mean of successive 3-month predictions from the 2nd to 4th lead month for each seasonal prediction. For example, summer mean prediction is calculated from the average of June, July and August forecasts integrating from May 1st.

3. Observed leading modes of the Asian-Australian monsoon system

Figure 1 shows the time series of the principal components (PCs) of the 1st and 2nd S-EOF mode obtained from the GPCP precipitation seasonal anomalies for the period 1979–2003. The PC time series exhibit remarkable interannual variations, which might be closely related to ENSO as measured by the Niño 3.4 SST anomalies. To examine their relationship with ENSO, the lead-lag correlation coefficients between the two PCs and the Niño 3.4 SST anomalies are presented in Fig. 2. Note that the A-AM precipitation seasonal anomaly from JJA(0) to the next MAM(1) is centered in November-December of year 0 (see Section 2; Yasunari, 1991). The observed first mode shows a maximum positive correlation coefficient that exceeds 0.9 with Niño 3.4 SSTA in D(0)JF(1). Since El Niño events normally mature toward the end of the calendar years (Rasmussen and Carpenter, 1982), the result in Fig. 2a indicates that the first S-EOF mode concurs with El Niño turnaround. On the other hand, the observed second mode shows a maximum correlation coefficient (0.75) leading El Niño by about one year, suggesting it may provide a precursory signal for ENSO onset (Fig. 2b).

Figure 3a shows the seasonal evolutions of the spatial patterns of A-AM precipitation anomalies associated with the first S-EOF mode. Also shown are the NCEP-2 850 hPa wind anomalies (vectors), which were linearly regressed against the corresponding first principal component in an enlarged domain including the entire tropical Indo-Pacific Oceans. In JJA (0) large-scale suppressed convections are located over the Maritime Continent and equatorial eastern Indian Ocean.

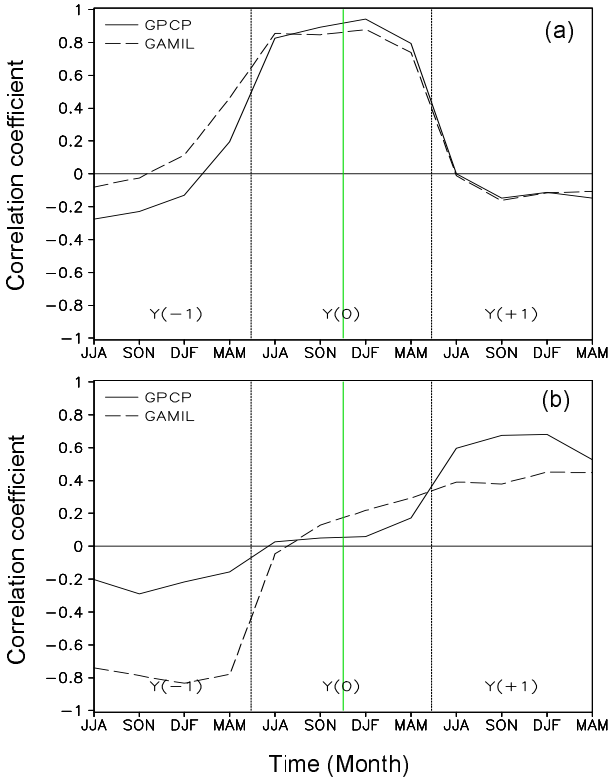

Fig. 2. (a) Lead-lag correlation coefficients between the first S-EOF principal component and the Niño 3.4 SST index. (b) The same as in (a) except for the 2nd S-EOF principal component.

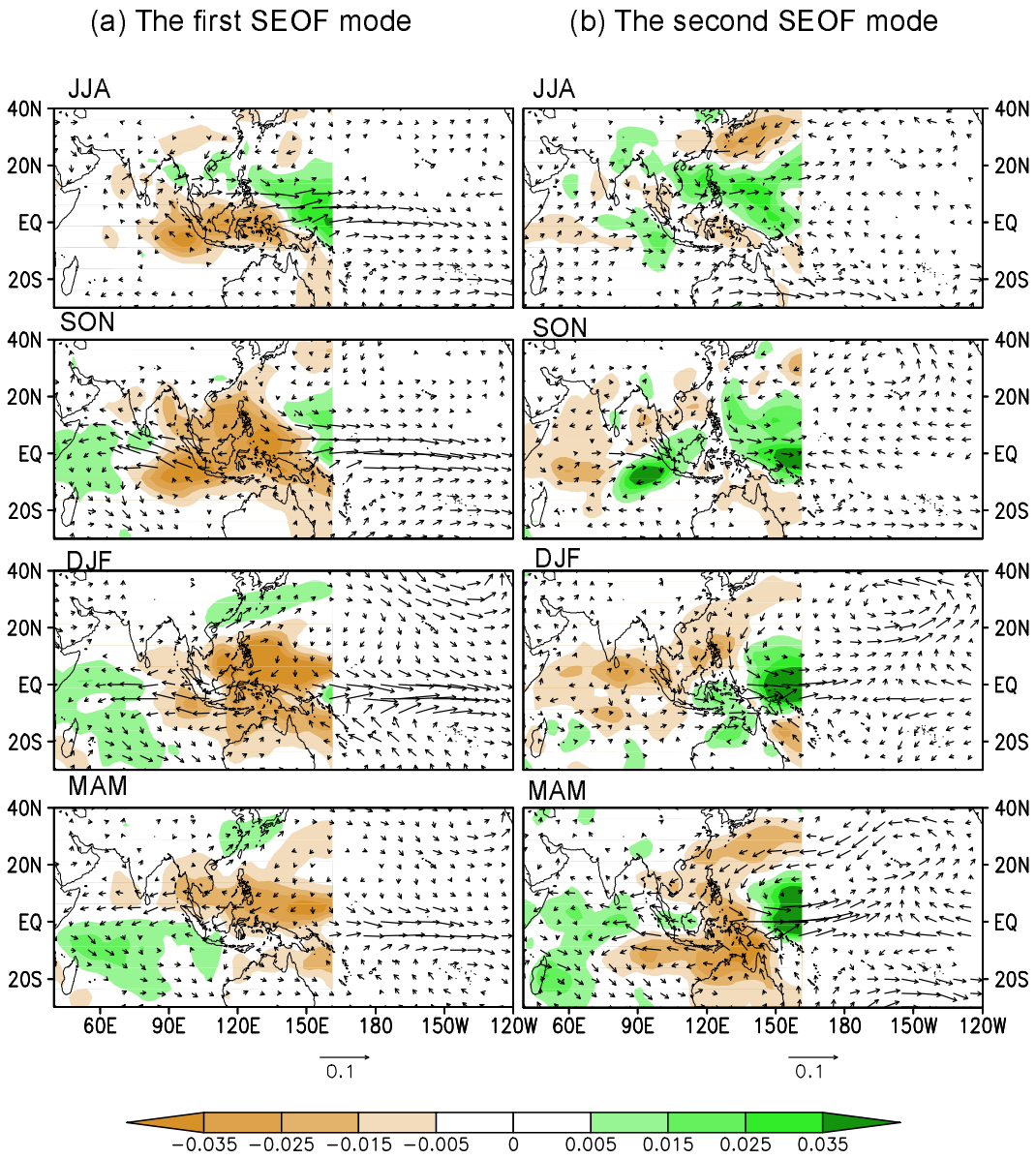

Fig. 3. Spatial patterns of the first S-EOF mode of seasonal precipitation anomalies from JJA(0) to MAM(1) (color shading, units: mm d^{-1}) and the NCEP-2 850 hPa wind anomalies (vectors, units: m s^{-1}), which were linearly regressed against the corresponding principal component. (b) Same as in (a) except for the 2nd S-EOF mode.

The dry anomalies extend northwestward to the southern Indian subcontinent and the Arabian Sea. The enhanced rainfall is found over the equatorial western Pacific. The wet anomalies also extend northwestward to the Philippine Sea, the northern South China Sea, and the Bay of Bengal. On the other hand, the precipitation along the East Asian monsoon front (Meiyu, Baiu and Changma) weakens. Associated with the anomalous convection patterns, an anomalous anticyclonic ridge extends from the Maritime Continent to the southern tip of India with enhanced monsoon westerlies extending from India to the western Pacific.

During SON(0), the dry anomalies over the Maritime Continent intensify and expand northward and eastward, which cover the Philippine archipelago and all of tropical South Asia and northern Australia. Meanwhile, the western Indian Ocean becomes wetter than normal and a dipole pattern develops in the tropical Indian Ocean. The corresponding Southern Indian Ocean (SIO) anticyclonic anomalies and the zonal wind divergence around the Maritime Continent are both well established. This pattern has been rec-

ognized as associated with the Indian Ocean zonal (or dipole) SST mode (Saji et al., 1999; Webster et al., 1999). From SON to DJF season, the anomalies move slowly eastward with the most suppressed convection shifting to the Philippine Sea. The SIO anticyclone weakens slightly, meanwhile a new anticyclonic anomaly forms over the Philippine Sea and southern China is controlled by southwesterly wind anomalies. The East Asian winter monsoon weakens but precipitation in southern China increases. From DJF to the next MAM, the dry anomalies decay rapidly and move further eastward with a dry center occurring in the equatorial western Pacific. The SIO and western North Pacific (WNP) anticyclones remain but weaken. The evolution of precipitation anomalies reflects their association with ENSO turnaround. The seasonal evolution of S-EOF 1 bears close resemblance to the leading mode of the season-dependent Singular Value Decomposition analysis of the tropical Pacific SST anomalies and the A-AM circulation anomalies derived by Wang et al. (2003).

Figure 3b shows spatial patterns of the second S-EOF mode. In SON(0), the fall prior to the El Niño development year, the WNP precipitation and cyclonic circulation anomaly pattern shift equatorward from their positions in the previous summer, and the convective dipole in the equatorial Indian Ocean intensifies. In the ensuing DJF and MAM, the anomalous WNP cyclone and associated equatorial westerly anomalies further strengthen, dominating the entire western Pacific region. At the same time, dry anomalies develop in the northern Indian Ocean and Southeast Asia in DJF and over eastern Indonesia and northern Australia in MAM (1). The anomalous pattern in MAM (1) is a robust precursor for El Niño development; it then evolves into a mature El Niño event in the central-eastern Pacific two or three seasons later.

Thus, an interesting precursory feature in the year prior to the ENSO event is that a large-scale cyclonic anomaly forms over the WNP in the summer to fall prior to the El Niño developing year. This is followed by a continuous southeastward movement and strengthening through the following fall, winter, and the next spring. This feature agrees well with the results of Wang (1995) who pointed out that this pattern has occurred since the late 1970s.

4. The major modes of A-AM variability in the GAMIL prediction

We first evaluate the skill of the one-month lead prediction of seasonal precipitation anomalies made by the GAMIL against the observed two leading modes, then compare them with those derived from GPCP observation in order to fully appreciate the model's skill. Furthermore, we also discuss major deficiencies with the GAMIL prediction.

Figure 1 shows that the temporal correlation coefficients between the observed and GAMIL predicted PC time series are about 0.91 for the first S-EOF mode and 0.32 for the second mode. Thus, the GAMIL predicted the temporal variations of the observed 1st mode very well, whereas the 2nd mode was not so well predicted. Further, Fig. 2 indicates that the GAMIL prediction captures, with high fidelity, the lead-lag correlations between ENSO and the 1st mode, while it fails to faithfully reflect the lead-lag correlations between ENSO and the 2nd mode. Note that the two observed leading modes of A-AM IAV are primarily associated with ENSO forcing and the local monsoon-warm ocean interaction. This implies that the A-AM IAV is basically determined by the ENSO forcing and the ENSO-excited local monsoon-warm ocean interaction. Land-sea thermal difference may be fundamental for seasonal time scales or annual cycles of A-AM rainfall but not for its IAV. These are consistent with the results obtained by Wang et al. (2003). Therefore, successful reproduction of the El Niño-excited monsoon-ocean interaction and El Niño forcing may be critical for the seasonal prediction of the IAV leading modes of the A-AM rainfall with the GAMIL.

The GAMIL's hindcast reproduces the major features of the observed first mode of the interannual variability of A-AM seasonal precipitation better than those of the second mode (Fig. 4). For the first S-EOF mode, the anomalous patterns are, in general, well forecast with the anomaly pattern correlation coefficient being 0.42. The second S-EOF mode patterns are not so well reproduced with the anomaly pattern correlation coefficient being 0.24. Larger discrepancies are primarily found over the joining area of Asia and the Indian-Pacific Ocean which includes the eastern Indian Ocean, the Maritime Continent, and the western Pacific warm pool. The low-level winds are not ideally reproduced in the tropics, especially in the Asian monsoon region during summer. As aforementioned, the local monsoon-ocean interactions over the joining area play an important role in the A-AM rainfall IAV, and the low prediction skill of the GAMIL may result from the deficiencies of reproduction in this joining area. Thus, simulation improvement in the joining area of Asia and the Indian-Pacific Ocean may be a crux of matter for improving the GAMIL prediction skill of the A-AM IAV.

Figure 5 shows the percentage variance accounted for by the first four eigenvalues of the S-EOF analysis of the A-AM precipitation. Shown also are the unit standard deviation of the sampling errors associated

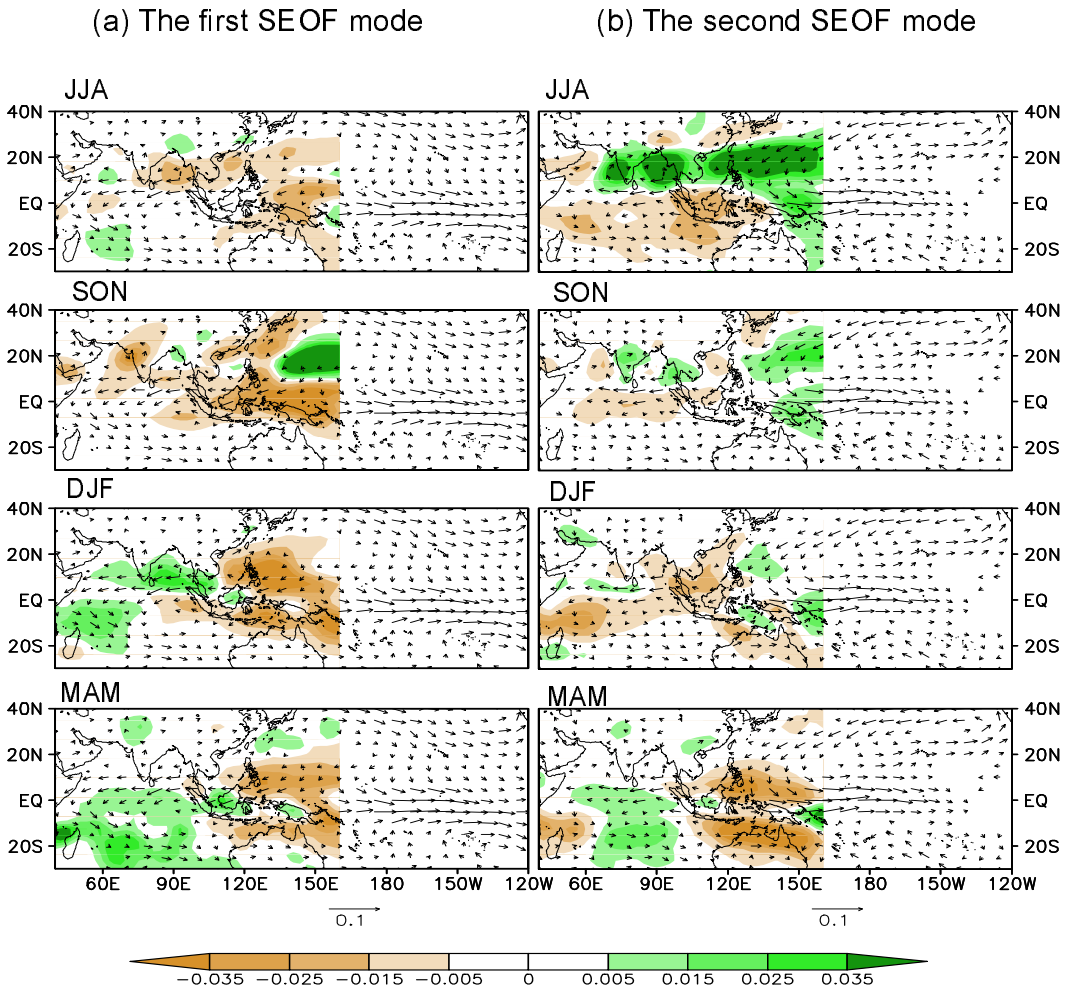

Fig. 4. (a) Comparison of the spatial patterns of the 1st S-EOF eigenvector of seasonal precipitation anomalies obtained from GPCP observation and GAMIL prediction. (b) The same as in (a) except for the 2nd S-EOF mode.

with each percentage eigenvalue. According to the rule of North et al. (1982), the observed first mode is well distinguished from the rest of the S-EOFs in terms of the sampling error bars. Hence, it is a statistically significant mode. The first two modes derived from the GAMIL prediction have similar levels of statistical significance as the observed counterparts, only with the fractional variance of the second mode slightly higher than that of the observed.

Since the ENSO-excited local atmosphere-warm ocean interaction is regarded as one of the physical factors that determine the variability of the A-AM, a feasible method for improving the GAMIL prediction in this area is to use one-tier prediction system which is considered to have taken into account local monsoon-warm pool ocean interactions (Wang et al., 2003; Wang et al., 2004a; Wu and Kirtman, 2005; Kumar et al., 2005). The coupled one-tier approach may enhance the predictability of the A-AM rainfall IAV.

5. Conclusion and discussion

Seasonal prediction of the A-AM precipitation is of central importance yet it is extremely challenging as far as climate prediction is concerned. Considering the A-AM anomalies vary strongly with season, an S-EOF analysis was adopted to depict the leading modes of the IAV. The S-EOF analysis of GPCP precipitation anomalies yields two distinguished modes. These two modes have distinct relationship with ENSO. The first mode concurs with the turnabout of warming (cooling) in the eastern-central Pacific, whereas the 2nd mode leads Niño 3.4 SST anomalies by about one year, providing a precursor for El Niño/La Niña development (Fig. 2).

The GAMIL which participated in APCC/CliPAS seasonal hindcast for the period 1979–2003 has been evaluated against the observed leading modes of the A-AM precipitation. It is found that the one-month

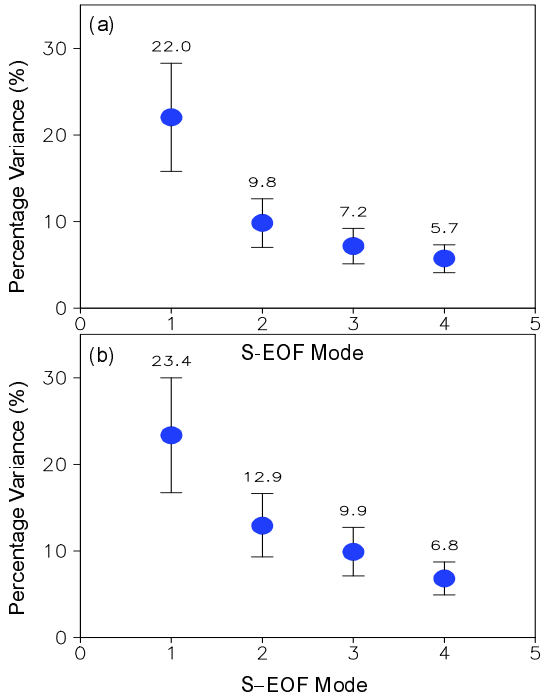

Fig. 5. Percentage variance (%) explained by the first 4 S-EOF modes of seasonal precipitation anomalies obtained from (a) GPCP and (b) GAMIL prediction. The bars represent one standard deviation of the sampling errors (North et al., 1982).

lead hindcast of the GAMIL is primarily able to capture major features of the observed two leading modes of the A-AM IAV, with the first mode better predicted than the second. It also depicts the relationship between the first mode and ENSO well. On the other hand, the GAMIL has deficiencies in capturing the relationship between the second mode and ENSO.

The GAMIL prediction discrepancies in the A-AM IAV basically come from the simulation biases in the joining area of Asia and the Indian-Pacific Ocean. Considering the fact that the El Niño-excited monsoon-ocean interaction and El Niño forcing may be critical for the A-AM rainfall IAV major modes, more efforts are needed to improve the simulation in the joining area of Asia and the Indian-Pacific Ocean as well as in the Niño 3.4 region. A feasible method is to employ a one-tier prediction system and the coupled one-tier approach which may enhance the predictability of the A-AM rainfall IAV. However, since the two leading IAV modes only explain 31.8% of the total variance, how to predict the A-AM rainfall IAV is still a challenging question.

In this study, we focus on the A-AM IAV prediction with the GAMIL. As a matter of fact, the A-AM variability has multi-timescale variations and the affecting factors will change if time scale changes. Then what factors contribute to the A-AM predictability on other time scales? In addition, since ENSO forcing and the ENSO-excited air-sea interaction play important roles in the A-AM rainfall anomalies' major modes, could we find any additional source of predictability for A-AM precipitation prediction? These are still open questions and need further investigations.

Acknowledgements. The authors acknowledge the support of the National Natural Science Foundation of China (Grant Nos. 40523001 and 40605022) and the Chinese Academy of the International Partnership Creative Group entitled "Climate System Model Development and Application Studies".

REFERENCES

Adler, R. F., and Coauthors, 2003: The Version 2 Global Precipitation Climatology Project (GPCP) Monthly Precipitation Analysis (1979–Present). *Journal of Hydrometeorology*, **4**, 1147–1167.

Bengtsson, L., U. Schlese, E. Roeckner, M. Latif, T. P. Barnett, and N. E. Graham, 1993: A two-tiered approach to long-range climate forecasting. *Science*, **261**, 1027–1029.

Cane, M. A., S. E. Zebiak, and S. C. Dolan, 1986: Experimental forecasts of El Niño. *Nature*, **321**, 827–832.

Kanamitsu, M. W. Ebisuzaki, J. Woolen, S-K. Yang, J. J. Hnilo, M. Fiorino, and G. L. Potter,, 2002: NCEP-DOE AMIP-II Reanalysis (R-2). *Bull. Amer. Meteor. Soc.*, **83**, 1631–1643.

Kim, K.-Y., 2002: Investigation of ENSO variability using cyclostationary EOFs of observational data. *Meteorology and Atmospheric Physics*, **81**, 149–168.

Kumar, K. K., M. Hoerling, and B. Rajagopalan, 2005: Advancing Indian monsoon rainfall predictions. *Geophys. Res. Lett.*, **32**, L08704, doi:10.1029/2004GL021979.

Li, L., B. Wang, Y. Wang, and H. Wan, 2007: Improvements in climate simulation with modifications to the Tiedtke Convective Parameterization in the Grid-point Atmospheric Model of IAP LASG (GAMIL). *Adv. Atmos. Sci.*, **24**, 323–335.

Li, J., and Q. Zeng, 2003: A new monsoon index and the geographical distribution of the global monsoons. *Adv. Atmos. Sci.*, **20**, 299–302.

Meehl, G. A., 1987: The annual cycle and interannual variability in the tropical Pacific and Indian Ocean regions. *Mon. Wea. Rev.*, **115**, 27–50.

North, G. R., T. L. Bell, R. F. Cahalan, and F. J. Moeng, 1982: Sampling errors in the estimation of empirical orthogonal functions. *Mon. Wea. Rev.*, **110**, 699–706.

Rasmussen, E. M., and T. H. Carpenter, 1982: Variations in tropical sea surface temperature and surface wind fields associated with the Southern Oscillation/El Niño. *Mon. Wea. Rev.*, **110**, 354–384.

Saji, H. N., B. N. Goswami, P. N. Vinayachandran, and T. Yamagata., 1999: A Dipole mode in the tropical

Indian Ocean. *Nature*, **401**, 360–363.

Smith, T. M., and R. W. Reynolds, 2004: Improved Extended Reconstruction of SST (1854–1997). *J. Climate*, **17**, 2466–2477.

Sperber, K. R., and T. N. Palmer, 1996: Interannual Tropical rainfall variability in general circulation model simulations associated with the Atmospheric Model Intercomparison Project. *J. Climate*, **9**, 2727–2750.

Tiedtke, M., 1989: A comprehensive mass flux scheme for cumulus parameterization in large-scale models. *Mon. Wea. Rev.*, **117**, 779–800.

Wang, B., 1995: Transition from a cold to a warm state of the El Niño-Southern Oscillation cycles. *Meteorology and Atmospheric Physics*, **56**, 17–32.

Wang, B., and S.-I. An, 2005: A method for detecting season-dependent modes of climate variability: S-EOF analysis. *Geophys. Res. Lett.*, **32**, L15710, doi:10. 1029/2005GL022709.

Wang, B., I.-S. Kang, and J.-Y. Lee, 2004a: Ensemble Simulations of Asian-Australian Monsoon Variability by 11 AGCMs. *J. Climate*, **17**, 803–818.

Wang, B., H. Wan, Z. Ji, X. Zhang, R. Yu, Y. Yu, and H. Liu, 2004b: Design of a new dynamical core for global atmospheric models based on some efficient numerical methods. *Science in China* (A), **47** (Suppl.), 4–21.

Wang, B., R. Wu, and T. Li, 2003: Atmosphere-Warm Ocean interaction and its impact on Asian-Australian Monsoon variation. *J. Climate*, **16**, 1195–1211.

Weare, B. C., and J. S. Nasstrom, 1982: Examples of extended empirical orthogonal function analyses. *Mon. Wea. Rev.*, **110**, 481–485.

Webster, P. J., V. O. Magana, T. N. Palmer, J. Shukla, R. A. Tomas, M. Yanai, and T. Yasunari, 1998: Monsoons: Processes, predictability, and the prospects for prediction. *J. Geophys. Res.*, **103**, 14451–14510.

Webster, P. J., A. M. Moore, J. P. Loschnigg, and R. R. Leben, 1999: Coupled ocean-atmosphere dynamics in the Indian Ocean during 1997–1998. *Nature*, **401**, 356–360.

Wu, R., and B. Kirtman, 2005: Roles of Indian and Pacific Ocean air-sea coupling in tropical atmospheric variability. *Climate Dyn.*, **25**, 155–170.

Yasunari, T., 1991: The monsoon year—A new concept of the climatic year in the Tropics. *Bull. Amer. Meteor. Soc.*, **72**, 1331–1338.

Zebiak, S. E., and M. A. Cane, 1987: A model El Niño southern oscillation. *Mon. Wea. Rev.*, **115**, 2262–2278.

Zhang, L., and J. Li, 2007: Seasonal rotation features of wind vectors and application to evaluate monsoon simulations in AMIP models. *Clim. Dyn.*, DOI 10.1007/s00382-007-0327-9.